Fermi National Accelerator Laboratory

Fermilab-Conf-86/130-T
September, 1986

# Resonant Neutrino Oscillations within the Solar Interior[1]

Stephen J. Parke

Fermi National Accelerator Laboratory
*P.O. Box 500, Batavia, Illinois, 60510*

## Abstract

Analytic results are derived for the electron neutrino survival probability after passage through a resonant oscillation region. This survival probability together with a sophisticated model of the production distribution of the solar neutrino sources and the solar electron number density are used to study the effects of resonant neutrino oscillation in the solar interior on the current and proposed solar electron neutrino experiments. The results are presented as contour plots for the electron neutrino capture rate, in the mass difference squared versus vacuum mixing angle plane, for the current $^{37}$Cl experiment and the proposed $^{71}$Ga detector.

[1]Invited talk at the XXIII International Conference on High Energy Physics, Berkeley, July 16-23, 1986.

# Resonant Neutrino Oscillations within the Solar Interior


**Stephen J. Parke**

Fermi National Accelerator Laboratory

*P.O. Box 500, Batavia, Illinois, 60510*



Analytic results are derived for the electron neutrino survival probability after passage through a resonant oscillation region. This survival probability together with a sophisticated model of the production distribution of the solar neutrino sources and the solar electron number density are used to study the effects of resonant neutrino oscillation in the solar interior on the current and proposed solar electron neutrino experiments. The results are presented as contour plots for the electron neutrino capture rate, in the mass difference squared versus vacuum mixing angle plane, for the current $^{37}$Cl experiment and the proposed $^{71}$Ga detector.


Recently, Mikheyev and Smirnov[1] have shown that the matter neutrino oscillations of Wolfenstein[2] can undergo resonant amplification in the solar interior thereby reducing the flux of electron neutrinos emerging from the Sun. This mechanism may be the solution to the solar neutrino puzzle[3,4]. Subsequently, Bethe[5] and others[6] have refined and restated the Mikheyev and Smirnov idea, pointing out that there are three general regions of parameter space in which the solar electron neutrino flux is sufficiently reduced. In this paper, I report an analytic result[7] for the electron neutrino survival probability after passage through a resonant oscillation region. Then, I outline a calculation[8] which uses this result, together with a relatively sophisticated solar model for the production distribution of solar neutrino sources and the solar electron number density, to generate contour plots of electron neutrino capture rates in the mass difference squared - vacuum mixing angle plane, for both chlorine ($^{37}$Cl) experiment and the proposed gallium ($^{71}$Ga) detector.

If neutrinos are massive then the flavor and mass eigenstates are not necessarily identical, however a general neutrino state can always be written in the flavor basis[9],

$$|\nu(t)\rangle = c_e(t)\,|\nu_e\rangle + c_x(t)\,|\nu_x\rangle\,. \tag{1}$$

In the ultra-relativistic limit, the evolution of this general neutrino state, in matter, is described by the following Schrodinger-like equation[2],

$$i\frac{d}{dt}\begin{pmatrix} c_e \\ c_x \end{pmatrix} = \frac{\Delta_N}{2}\begin{pmatrix} -\cos 2\theta_N & \sin 2\theta_N \\ \sin 2\theta_N & \cos 2\theta_N \end{pmatrix}\begin{pmatrix} c_e \\ c_x \end{pmatrix}. \tag{2}$$

With $\Delta_N$ and $\theta_N$ determined by

$$\begin{aligned}\Delta_N \cos 2\theta_N &= \frac{\delta m^2}{2k}\cos 2\theta_0 - \sqrt{2}G_F N_e,\\ \Delta_N \sin 2\theta_N &= \frac{\delta m^2}{2k}\sin 2\theta_0\end{aligned}$$

where $\delta m^2 \equiv (m_2^2 - m_1^2)$, $m_i$ are the neutrino masses, k is the neutrino energy, $\theta_0$ is the vacuum mixing angle, $G_F$ is the Fermi constant and $N_e$ is the electron number density. The constraints $\delta m^2 > 0$ and $\theta_0 < \pi/4$ are assumed.

At an electron density, $N_e$, the matter mass eigenstates are

$$\begin{aligned}|\nu_1, N\rangle &= \cos\theta_N\,|\nu_e\rangle - \sin\theta_N\,|\nu_x\rangle\\ |\nu_2, N\rangle &= \sin\theta_N\,|\nu_e\rangle + \cos\theta_N\,|\nu_x\rangle\end{aligned} \tag{3}$$

which have eigenvalues $E_1 = -\Delta_N/2$ and $E_2 = \Delta_N/2$. At resonance, the electron density is given by $N_e^{res} = \delta m^2 \cos 2\theta_0 / 2\sqrt{2} k G_F$, and the matter mixing angle $\theta_N^{res} = \pi/4$. Above resonance, $\theta_N$ satisfies $\pi/4 < \theta_N \leq \pi/2$.

For a constant electron density these matter mass eigenstates evolve in time by the multiplication of a phase factor. Also, for a slowly varying electron density, these states evolve independently in time; that is $e^{-i\int^t E_1 dt}\,|\nu_1, N(t)\rangle$ and $e^{-i\int^t E_2 dt}\,|\nu_2, N(t)\rangle$ are the adiabatic states. Therefore, it is convenient to use these states, as the basis states, in the region for which there are no transitions (away from the resonance region). As a neutrino goes through resonance these adiabatic states maybe mixed, but on the other side of resonance, the neutrino state can still be written as a linear combination of these states. That is, a basis state produced at time $t$, going through resonance at time $t_r$, and detected at time $t'$ is described by

$$e^{-i\int_t^{t_r} E_1 dt}\,|\nu_1, N(t)\rangle \rightarrow$$

$$a_1\, e^{-i\int_{t_r}^{t'} E_1 dt}\,|\nu_1, N(t')\rangle \;+\; a_2\, e^{-i\int_{t_r}^{t'} E_2 dt}\,|\nu_2, N(t')\rangle$$

or

$$e^{-i\int_t^{t_r} E_2 dt}\,|\nu_2, N(t)\rangle \rightarrow$$

$$-a_2^*\, e^{-i\int_{t_r}^{t'} E_1 dt}\,|\nu_1, N(t')\rangle \;+\; a_1^*\, e^{-i\int_{t_r}^{t'} E_2 dt}\,|\nu_2, N(t')\rangle$$

where $a_1$ and $a_2$ are complex numbers such that $|a_1|^2 + |a_2|^2 = 1$. The relationship between the coefficients, for these two basis states, is due to the special nature of the wave equation, eqn(2). The phase factors have been chosen so that coefficients $a_1$ and $a_2$ are characteristics of the transitions at resonance and are not related to the production and detection of the neutrino state.

The detection averaged electron neutrino survival probability is easily calculated as

$$\begin{aligned} P_{\nu_e}(t) &= \frac{1}{2} + \frac{1}{2}(|a_1|^2 - |a_2|^2)\cos 2\theta_N \cos 2\theta_0 \\ &- |a_1 a_2| \sin 2\theta_N \cos 2\theta_0 \cos(\int_{t_r}^{t} \Delta_N dt + \omega)) \end{aligned}$$

with $\omega = \arg(a_1 a_2)$. The last term shows that the phase of the neutrino oscillation at the point the neutrino enters resonance can substantially effect this probability. Therefore, we must also average over the production position, to obtain the fully averaged electron neutrino survival probability[7,10] as

$$\overline{P_{\nu_e}} = \frac{1}{2} + (\frac{1}{2} - P_x)\cos 2\theta_N \cos 2\theta_0 \qquad (4)$$

where $P_x = |a_2|^2$, the probability of transition from $|\nu_2, N>$ to $|\nu_1, N>$ (or vice versa ) during resonance crossing. The non-resonant crossing case is trivially obtained by setting $P_x = 0$.

Similar calculations can also be performed for the case of double resonance crossing (neutrinos from the far side of the sun). Here we must average not only over the production and detection positions of the neutrino but also over the separation between resonances. This sensitivity to the separation of the resonances can be understood as the effect of the phase of the oscillation as the neutrino enters the second resonance region. The fully average probability of detecting an electron neutrino is the same as eqn(4) with $P_x$ replaced by $P_{1x}(1 - P_{2x}) + (1 - P_{1x})P_{2x}$ (the classical probability result). Therefore, the generalization to any number of resonance regions, suitable averaged, is obvious.

To calculate the probability, $P_x$, the approximation that the density of electrons varies linearly in the transition region is used. That is, a Taylor series expansion is made about the resonance position and the second and higher derivative terms are discarded. In this approximation the probability of transition between adiabatic states was calculated by Landau and Zener. This is achieved by solving the Schrodinger equation, eqn(2), exactly in this limit. Applying their result to the current situation[7,11] gives

$$P_x = \exp\left[-\frac{\pi}{2}\frac{\sin^2 2\theta_0}{\cos 2\theta_0}\frac{\delta m^2/2k}{|\vec{n}\cdot\nabla \ln N_e|_{res}}\right] \qquad (5)$$

where the unit vector, $\vec{n}$, is in the direction of propagation of the neutrino. Eqn(4) and (5) demonstrate that only the electron number density, at production, and the logarithmic derivative of this density, at resonance, determine the electron neutrino survival probability. For a discussion of the range of validity of this approximation see ref(7).

Before applying these results to the solar model in detail, let us first consider an exponential electron number density profile which is a good approximation for the solar interior except near the center. In figure (a), I have plotted the electron neutrino survival probability contours at the earth in the $\delta m^2/2\sqrt{2}kG_F N_c$ versus $\sin^2 2\theta_0/\cos 2\theta_0$ plane for such an exponential density profile. Here, the Solar central electron number density, $N_c$, is also the number density at the point where the neutrinos are produced. This plot depends only on the properties of the sun and this dependency is through the combination $R_s N_c$, where $R_s$ is the scale height. For this figure, I have used an $N_c$ corresponding to a density of 140g cm$^{-3}$ and $Y_e = 0.7$ and a scale height $R_s$ of 0.092 times the radius of the sun.

Above the line $\delta m^2/2\sqrt{2}kG_F N_c = 1/\cos 2\theta_0$ in this plot, the neutrinos never cross the resonance density on there way out of the sun. Here, the probability of detecting an electron neutrino is close to the standard neutrino oscillation result. Below this line, the effects of passing through resonance comes into play. Inside the 0.1 contour "triangle", there is only a small probability of transitions between the adiabatic states as the neutrino passes through resonance. To the right of this contour triangle, the probability of detecting a neutrino grows, not because of transitions, but because both adiabatic states have a substantial mixture of electron neutrino at zero density. To the left and below the 0.1 contour triangle, the probability grows because here there are significant transitions between the adiabatic states as the neutrino crosses resonance.

More precisely, the solar electron neutrino capture rate for a detector characterized by a electron neutrino capture cross section, $\sigma(E)$, and energy threshold $E_0$, is

$$\sum_{\text{processes}} \int_{E_0}^{\infty} \frac{d\Phi_\nu}{dE}\sigma(E)dE. \qquad (6)$$

The sum is taken over all neutrino sources in the Sun and $d\Phi_\nu/dE$ is the differential electron neutrino flux of a given source at the earth's surface. To include the reduction in the electron neutrino flux from the Sun due to resonant neutrino oscillations, the differential electron neutrino flux for each process was calculated as

$$\frac{d\Phi_\nu}{dE} \propto W(E) \int_{sun} dV\ \overline{P_{\nu_e}} \frac{df}{dV} \qquad (7)$$

where W(E) is the standard weak interaction energy distribution for the neutrinos of a given process and df/dV is the fraction of the standard solar model flux coming from a given solar volume element for this process. The values of df/dV for the various processes and from Bahcall's solar model[12]. $d\Phi_\nu/dE$ was normalized for each process by demanding that the energy and solar volume integrations of eqn(6) yield the capture rates given in the Table[4], when $\overline{P_{\nu_e}} = 1$. Details of the cross sections used can be found in ref(8).

Neutrino Sources and Capture Rates (SNU)

| Process | $E_\nu^{max}$(MeV) | $^{37}$Cl | $^{71}$Ga |
|---|---|---|---|
| $^8$B | 14.06 | 4.3 | 16 |
| $^7$Be | 0.861(90%) +0.383(10%) | 1.0 | 27 |
| p-p | 0.420 | 0 | 70 |
| pep | 1.44 | 0.23 | 2.5 |
| $^{13}$N | 1.199 | 0.08 | 2.6 |
| $^{15}$O | 1.732 | 0.26 | 3.5 |
| Total | | 5.9 | 122 |

In figures (b) and (c), we present electron neutrino capture rate contours (iso-SNU contours) for the $^{37}$Cl and $^{71}$Ga experiments as a function of $\delta m^2$ and $\sin^2 2\theta_0/\cos 2\theta_0$ for this solar model. The $3\sigma$ deviations from the Davis *et al.*[3] result of 2.1 SNU are the 2.4 and 1.8 iso-SNU contour lines in figure (b). The generic structure of these total SNU plots is due to the superposition of triangular iso-SNU contours associated with each individual neutrino source contributing to a given total SNU value. These individual contours owe their shape to the appropriate iso-probability contour, figure (a), and their position is determined by the typical energy scale and production electron density of the individual neutrino source. For each neutrino source the resonance mechanism becomes important, provided $\theta_0 > 0.01$, as soon as $\delta m^2$ becomes small enough so that the average resonant electron density for that source is less than the solar electron density at the production site. This occurs when $\delta m^2$ is approximately equal to $1.5 \times 10^{-4}$, $1.2 \times 10^{-5}$, and $3.7 \times 10^{-6}$ eV$^2$ for the $^8$B, $^7$Be and pp neutrinos respectively. Below these values the individual neutrino sources have contours which are diagonals of slope minus one coming from the form of the transition probability between adiabatic states, eqn(5). The intersection of these diagonal lines with the turning on of resonance for $^8$B, $^7$Be and pp is responsible for the shoulders at small $\sin^2 2\theta_0/\cos 2\theta_0$ in the contour plots. The vertical sections of the contours, at large $\theta_0$, occur because for large $\theta_0$ both adiabatic states have a large component of electron neutrino.

From figure(c), we see that the results of the $^{71}$Ga experiment can range from 10 to 110 SNU and still be compatible with the $^{37}$Cl experiment. In general, a given gallium contour crosses the $2.1 \pm 0.3$ chlorine contour at least twice and therefore the results of the $^{71}$Ga experiment will leave a two-fold degeneracy in $(\delta m^2, \theta_0)$-space. If one accepts the theoretical prejudice against large vacuum angles provided by see-saw

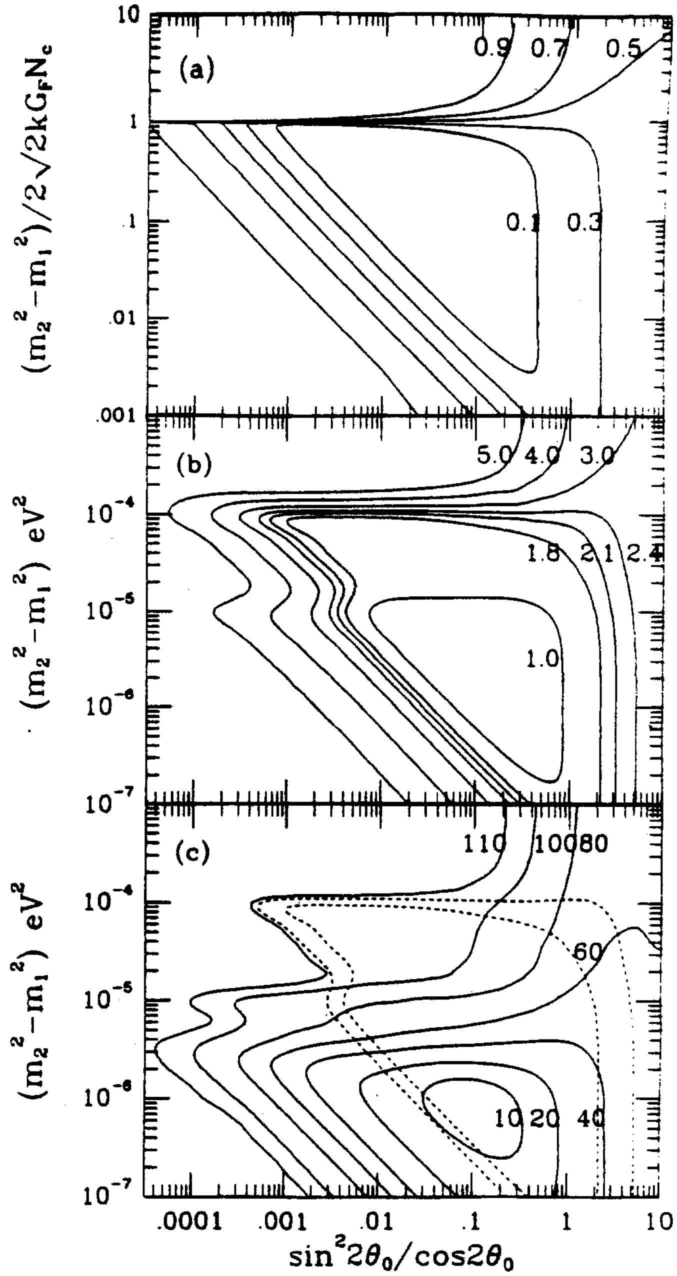


Figure (a): Electron neutrino survival probability contours for an exponential solar electron density profile and an electron neutrino produced at center of the Sun.

(b): Iso-SNU contours for the $^{37}$Cl experiment using Bahcall's solar model. The contours are labeled with their the corresponding SNU values.

(c): Iso-SNU contours for a $^{71}$Ga detector using Bahcall's solar model. The solid contours are labeled with their appropriate $^{71}$Ga SNU values and the dashed contours are the $3\sigma$ deviations from the Davis $^{37}$Cl experimental result.

models[13], this degeneracy is removed. Unfortunately, the degeneracy is continuous for that region of parameter space corresponding to a $^{37}$Cl rate of 2.1 $\pm$ 0.3 SNU and a $^{71}$Ga rate greater than 100 SNU. In this region *only* the $^{8}$B neutrinos are effected by the resonance phenomena. Also, in this region of parameter space the two experiments will not be able to distinguish between a small temperature change at the solar core and the resonant neutrino oscillation mechanism. This is due to the relatively strong temperature dependence of the $^{8}$B neutrino flux[14]. It is only when the $^{71}$Ga SNU rate is depleted below that of merely removing the $^{8}$B component (*i.e.*, appreciably less than 110 SNU), so that reduction of the less temperature sensitive neutrinos ($^{7}$Be and pp) becomes necessary, that the resonant oscillation mechanism becomes a likely solution to the solar neutrino problem.

Finally, I would like to thank my collaborator Terry Walker.

## References

1. S.P. Mikheyev and A.Yu. Smirnov, *10th International Workshop on Weak Interactions and Neutrinos*, Savonlinna, Finland(1985); *Nuovo Cimento* **C9**, 17(1986).

2. L. Wolfenstein, *Phys. Rev.* **D17**, 2369(1978); *Phys. Rev.* **D20**, 2634(1979).

3. R. Davis, D.S. Harmer, and K.C. Hoffman, *Phys. Rev. Lett.* **20**, 1205(1968).

4. J.N. Bahcall, B.T. Cleveland, R. Davis, and J.K. Rowley, *Astrophys. J.* **292**, L79(1985).

5. H.A. Bethe, *Phys. Rev. Lett.* **56**, 1305(1986).

6. A. Messiah and S.P. Rosen and M. Spiro, *1986 Massive Neutrinos in Astrophysics and in Particle Physics*, Tignes, January 1986; S.P. Rosen and J.M. Gelb, *Phys. Rev.* , **D34**, 969(1986); E.W. Kolb, M.S. Turner, and T.P. Walker, Phys. Lett., **B175**, 478(1986); V. Barger, R.J.N. Phillips, and K. Whisnant, *Phys. Rev.* , D34, 980(1986).

7. S.J. Parke, *Phys. Rev. Lett.* **57**, 1275(1986).

8. S.J. Parke and T.P. Walker, *Phys. Rev. Lett.* (to be published).

9. The other flavor eigenstate could $\nu_\mu$ or $\nu_\tau$.

10. A. Messsiah, *1986 Massive Neutrinos in Astrophysics and in Particle Physics*, Tignes, January 1986.

11. W.C. Haxton, *Phys. Rev. Lett.* **57**, 1271(1986).

12. J.N. Bahcall, W.F. Huebner, S.H. Lubow, P.D. Parker, and R.K. Ulrich, *Rev. Mod. Phys.* **54**, 767(1982).

13. T. Yanagida, *Prog. Theor. Phys.* **B135**, 66(1978); M. Gell-Mann, P. Ramond, and R. Slansky, in *Supergravity*, eds. P. van Nieuwenhuizen and D. Freedman, (North Holland)(1979).

14. In the case where a $^{71}$Ga rate of $\gtrsim$ 100 SNU is measured, a measurement of the $^{8}$B solar neutrino spectrum (see Rosen and Gelb ref. 6) or the flavor independent solar neutrino flux (see S. Weinberg, contribution to this proceedings) would allow us to distinguish between changes in the solar model and resonant neutrino oscillations.